Korean J. Chem. Eng., 33(5), 1743-1748 (2016)
DOI: 10.1007/s11814-016-0017-6

pISSN: 0256-1115
eISSN: 1975-7220

Superhydrophobic, flexible and gas-permeable membrane prepared by a simple one-step vapor deposition

Bo Ra Kim, Dae Han Kim, and Young Dok Kim†

Department of Chemistry, Sungkyunkwan University, Suwon 16419, Korea
(*Received 7 November 2015 • accepted 17 January 2016*)

Abstract−We demonstrate the fabrication of superhydrophobic, flexible and gas-permeable membranes by a simple one-step process consisting only of thermal evaporation of a fluid polydimethylsiloxane (PDMS) polymer, without the use of any other chemicals such as curing agents or solvents of PDMS. As a substrate for the PDMS coating, a stainless steel mesh approx. 100 μm thick was used, which is flexible and becomes superhydrophobic after PDMS coating, attaining a water contact angle above 160°. The flexible mesh remained gas-permeable upon superhydrophobic coating, since PDMS evenly coated each strand of the metal mesh, and the vacancies between wires remained unclogged upon coating. The mechanical and chemical stability of the superhydrophobic, flexible and gas-permeable membrane is demonstrated herein.

Keywords: Superhydrophobicity, Chemical Vapor Deposition, Polydimethylsiloxane, Gas Permeability, Flexibility

INTRODUCTION

Superhydrophobicity is the phenomenon whereby a water droplet on a solid surface shows a contact angle exceeding 150° and an extremely low sliding angle (typically less than 5°) [1-7]. A water droplet can easily roll over the surface of a superhydrophobic material, thereby sweeping away dust particles in a so-called self-cleaning process that also occurs on lotus leaves in nature. Superhydrophobicity has been one of the most widely studied subjects in material science and technology in recent decades, and its microscopic origin is relatively well understood: it results from surface termination with hydrophobic functionality such as alkyl or fluoroalkyl groups, coupled with a unique geometric surface structure consisting of superposed microscale and nanoscale roughness [1,8-15]. A water droplet in contact with a hydrophobic surface with such dual surface roughness does not easily wet the surface but is repelled by air pockets at the water/solid interface.

Many strategies for the fabrication of superhydrophobic surfaces have been developed so far. One can use lithographic techniques to make hierarchical surface structures, and then cover them with hydrophobic molecules [16-18]. One can also prepare superhydrophobic structures by self-assembly techniques using hydrophobic or hydrophobically modified nanoparticles; appropriately selected nanoparticles coated on a solid surface will spontaneously form the requisite structure of dual roughness, with microscale roughness arising from the agglomeration of nanoparticles, and nanoscale roughness arising from the individual nanoparticles [19-21]. Among the various methods for the deposition of hydrophobic nanoparticles onto the surface in such techniques, aerosol deposition is often used [22-26]. In this method, a hydrophobic polymer such as polydimethylsiloxane (PDMS) is dissolved in a solvent (e.g., chloroform) and ultrasonically evaporated to form an aerosol precursor which is then delivered by a carrier gas and deposited on the surface.

In the present work, we show that a superhydrophobic surface can be prepared by simple vapor deposition of PDMS without using any other chemicals, such as curing agents or additional solvents, and without the use of any physical or chemical treatments other than the thermal heating of PDMS. It is first time to use direct evaporation of PDMS to a flat substrate to form superhydrophobic layer instead of using nanostructured substrate surfaces. As an example of this technique, we prepared a superhydrophobic coating on a flexible and gas-permeable metal mesh.

EXPERIMENTAL

1. Materials

Fluid PDMS (Dow Corning, Sylgard 184) and acetone (Daejung, 99.5%) were used as received. The average molecular weight (Mn), weight average molecular weight (Mw) and polydispersity index (PDI) of PDMS were 4,200 g·mol^{-1}, 14,000 g·mol^{-1} and 3.3, respectively (measured by gel permeation chromatography; Agilent Technologies, Agilent 1100s) [27]. Stainless steel mesh of wire diameter 53 μm and having rectangular pores 100 μm square was provided by Ehwa Chulmang.

2. Preparation of the Superhydrophobic Mesh Film

Before PDMS coating, the stainless steel mesh substrate was cleaned in acetone for 15 min and dried with a heat gun for 1 min. Superhydrophobic mesh film was prepared by a one-step vapor deposition method, as follows: the bare mesh and fluid PDMS source (16 g) were physically separated inside a stainless steel reactor, and the reactor was sealed with polyimide (PI) tape (Fig. 1). The distance between the metal mesh and the PMDS-container was approx. 7 cm. The reactor was equipped with a power supply, a k-type thermocouple, a heating band and a temperature controller.

†To whom correspondence should be addressed.
E-mail: ydkim91@skku.edu
Copyright by The Korean Institute of Chemical Engineers.

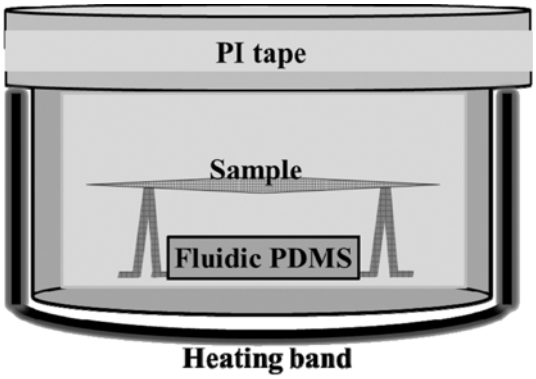

Fig. 1. Schematic description of the stainless steel reactor showing the position of stainless steel mesh (sample) and fluidic PDMS during chemical vapor deposition.

The reactor was heated at 300 °C for 8 h to carry out the coating. Note that the chamber wall, which was close to the PDMS precursor, was set at 300 °C; however, the substrate (metal mesh) was located in the middle of the reactor with a temperature of ~200 °C, which is lower than the chamber wall temperature. PDMS evaporates at 300 °C, and these vapor species are deposited on the metal mesh at ~200 °C.

3. Characterization

Water contact angle measurements were conducted using a Theta optical tensiometer (KSV Instruments, Ltd.) equipped with a digital camera connected to a computer; Young-Laplace curves were employed to carry out the fitting process required for determining contact angles. Water droplets of approx. 5 µl were used to measure the static water contact angle (θ_{sta}). Contact angle hysteresis (θ_{hys}) was examined by subtracting the receding contact angle (θ_{re}) from the advancing contact angle (θ_{ad}); θ_{ad} is the maximum contact angle obtained upon adding water to the droplet, whereas θ_{re} is the minimum contact angle observed upon withdrawing water from the droplet. All water contact angles reported were determined by averaging the results measured at three different positions on a sample. Chemical structural characterization of bare and PDMS-coated samples was by Fourier transform infrared (FT-IR) spectroscopy (BRUKER, Optics/vertex 70). The surface morphologies of the mesh before and after PDMS coating were imaged at various magnifications by means of scanning electron microscopy (SEM, JEOL, JSM-7100F).

4. Mechanical and Chemical Stability of Superhydrophobic Surfaces

To evaluate the chemical stability of the superhydrophobic surfaces, specimens of PDMS-coated mesh were exposed to acidic (HCl (aq), pH 2.5) and basic (NaOH (aq), pH 12) aqueous solutions for 40 min. In addition, the photostability of the coated mesh surface was evaluated by means of a 12 h UV light irradiation test (Vilber Lourmat UV lamp, λ=254 nm). A sand abrasion test was performed to evaluate the mechanical resistance of the superhydrophobic surfaces: in each test, 20 g of sand (average particle size of 100 µm) was dropped from a height of 30 cm onto a mesh surface, which was tilted at the angle of 45°. The velocity of the dropped sand was about 0.22 $m \cdot s^{-1}$ (Fig. 2(a)).

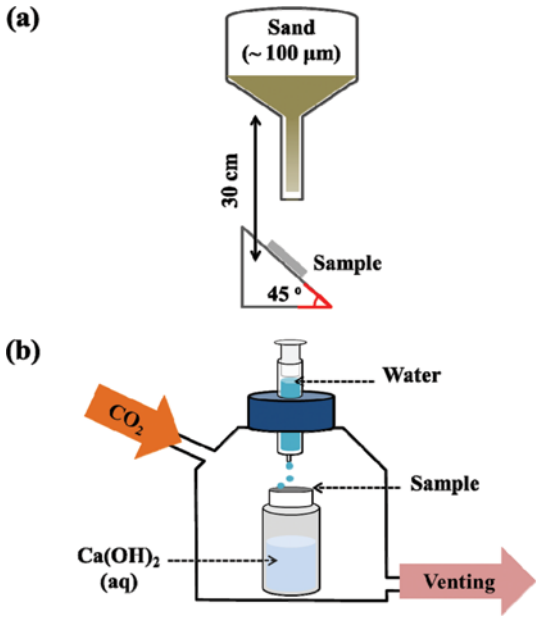

Fig. 2. (a) Schematic description of the sand abrasion test apparatus showing the position of sand and PDMS-coated mesh (sample) during the abrasion test. (b) Schematic description of the glass reactor showing the position of vial wrapped with a PDMS-coated mesh (sample), syringe containing distilled water dyed with methylene blue and direction of CO_2 gas flow.

5. Gas Permeation and Water Repellency Test of Superhydrophobically Coated Mesh

Gas permeation testing was carried out using a $CaCO_3$ precipitation reaction (Fig. 2(b)). A vial was labelled by affixing printed letters to its sidewalls, and $Ca(OH)_2$ aqueous solution (3.2 mM) was added to the vial such that the letters could be seen. The mouth of the vial was wrapped with a PDMS-coated mesh and then the vial was placed in a glass reactor with branches to allow CO_2 gas flow (30 pounds per square inch). CO_2 that permeated into the aqueous solution reacted with $Ca(OH)_2$ to form $CaCO_3$ precipitation, whereby a clear aqueous solution would become hazy. After the gas permeation testing, distilled water dyed with methylene blue was dropped onto the PDMS-coated mesh sample using a syringe that was fixed at the cover of the glass reactor. The water repellency of the mesh sample was then examined by observing the action of the water droplet on the surface.

RESULTS AND DISCUSSION

1. Characterization of Bare and PDMS-coated Meshes

The wetting of bare and PDMS-coated meshes was studied by measuring the static water contact angle (θ_{sta}) and the contact angle hysteresis (θ_{hys}). The bare mesh had a static water contact angle of 113.3°; the static water contact angle of the PDMS-coated mesh was about 50° higher. Also, the contact angle hysteresis of the PDMS-coated mesh was below 5° (Table 1). Thus, it was confirmed that the mesh surface became superhydrophobic after the PDMS coating process, which means that a change in chemical structure and

Table 1. Static water contact angles (θ_{sta}) of bare and PDMS-coated meshes and water contact angle hysteresis values (θ_{hys}) of PDMS-coated mesh. Optical pictures showing the shape of water droplet on bare and PDMS-coated meshes are also presented

Sample	Bare	PDMS-coated	
	θ_{sta}	θ_{sta}	θ_{hys}
Mesh	113.3° 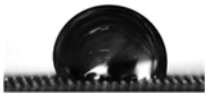	162.3° 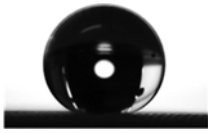	4.6°

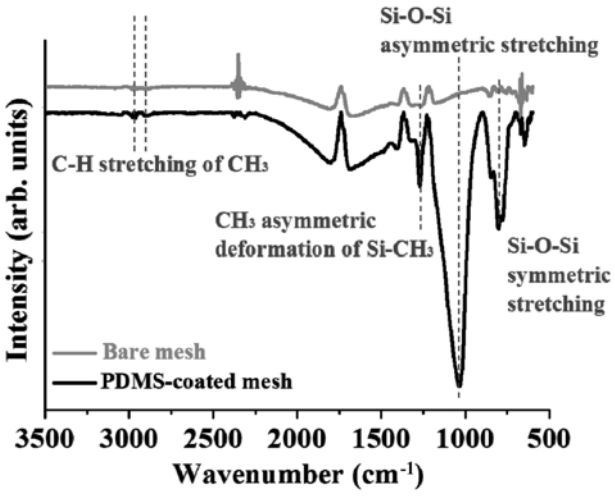

Fig. 3. FT-IR spectra of bare and PDMS-coated meshes.

surface morphology on the mesh surface occurred.

The chemical structures of bare and PDMS-coated meshes were identified using FT-IR analysis. Several new vibrational peaks were clearly evident in the FT-IR spectrum of the PDMS-coated mesh (Fig. 3). Peaks observed at 800 cm^{-1} and 1,039 cm^{-1} were attributed to the characteristic absorption bands of Si-O-Si symmetric and asymmetric stretching, respectively [28]. A peak at approx. 1,260 cm^{-1} was attributed to CH_3 symmetric deformation in Si-CH_3 [29 30], and peaks located at 2,968 and 2,900 cm^{-1} were respectively attributed to the asymmetric and symmetric stretching of sp^3 C-H [31]. Based on the FT-IR results, one can suggest that the chemical structure of the deposited layer on PDMS-coated mesh consisted of a dimethylsiloxane network of PDMS, providing a hydrophobic functionality on the mesh surface [32-36].

The surface morphology of bare and PDMS-coated meshes was studied by analyzing SEM images (Fig. 4). The bare mesh had a smooth wire surface with a wire diameter of approx. 100 μm, and rectangular pores of side length comparable to the wire diameter (Fig. 4(a) and (b)). Contrastingly, the PDMS-coated mesh was highly rough over the entire wire surface (Fig. 4(d)). Most of the PDMS-coated mesh surface was evenly covered by particles several hundreds of nanometers in size, and a sparse distribution of larger particles in the size range of several micrometers was also observed, most

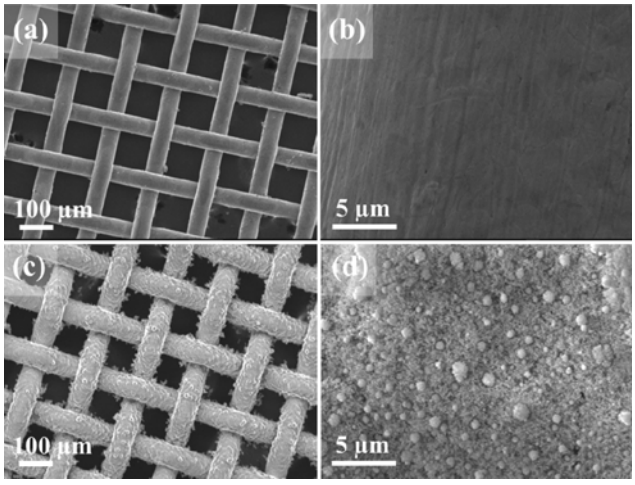

Fig. 4. SEM images of (a), (b) bare mesh and (c), (d) PDMS-coated mesh; (b) and (d) are magnified views.

likely corresponding to agglomerations of smaller nanoparticles.

A hierarchical structure formed by the superposition of dense nanostructures and micrometer-sized particles of PDMS can produce superhydrophobicity [37,38]. Most likely, PDMS vapor evaporated in the sealed reactor agglomerated in the vapor phase into aerosol particles, thereby forming upon deposition the rough surfaces observed. The micrometer-scale roughness caused by deposition of PDMS vapor on mesh substrate induced superhydrophobic surface, which means that PDMS-coated mesh has anti-wetting property. It is also notable that the apertures of the mesh pores remained fully unclogged after the coating process, allowing gas to pass freely through the PDMS-coated mesh.

Note that selection of a PDMS deposition temperature lower than 300 °C could not produce such a superhydrophobic surface structure. The deposition temperature could not exceed 300 °C, since at these temperatures, SUS reactor can be oxidized and PDMS precursor can be burned.

To shed more light on the mechanism of the formation of hydrophobic layers in our experiment, we performed pyrolysis gas chromatography-mass spectroscopy (GC-MS) analyses of the species vaporized from PDMS heated at 300 °C (Fig. S1). We found that the species actually vaporized from our PDMS are mainly the species with relatively low molecular weights (below 400 amu): the major vapor species are relatively low-molecular-weight siloxane such as pentasiloxane. Even though there are also species vaporized during heating PDMS at 300 °C other than these siloxane species, we suggest, based on the pyrolysis GC-MS data, that the relatively low-molecular weight siloxane species are vaporized and deposited on the metal mesh surface, forming superhydrophobic thin films. Another possible path for the hydrophobization is that the silanol species, which are formed by decomposition of PDMS during heating PDMS (which was also detected with less abundance than the siloxane in the pyrolysis GC-MS data) undergo condensation reaction on metal mesh surface and form hydrophobic layer.

2. Stability of Superhydrophobic Surface on PDMS-coated Mesh

To study the mechanical stability of the superhydrophobic surfaces formed by our vapor deposition method, PDMS-coated meshes

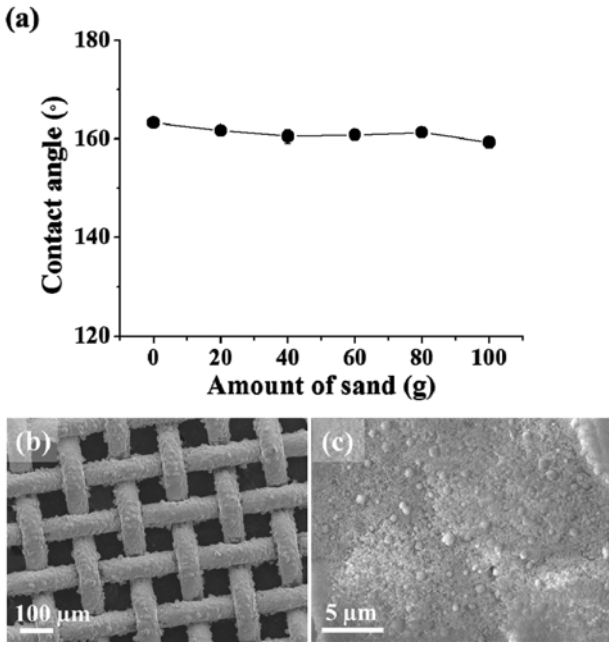

Fig. 5. Results of the sand abrasion test of PDMS-coated mesh: (a) change in water contact angle of PDMS-coated mesh as a function of amount of fallen sand, (b) SEM images of the coated mesh after sand abrasion test.

were subjected to a sand abrasion test. Note that the organic molecules such as stearic acid widely used for the hydrophobization of the surface suffer from low stability under acidic and basic conditions and UV irradiation, which is regarded as hurdle of application of superhydrophobic surfaces. For application of the superhydrophobic layers, chemical, and mechanical durability of the layer should be warranted [32,33]. For example, gas permeable superhydrophobic layer can be used as a shielding layer of chemical gas sensor, which can allow selective permeation of gas and repel aqueous solutions for protection of the gas sensor. For such application, chemical and mechanical durability of the superhydrophobic layer is of importance.

Fig. 5(a) shows the static water contact angle as a function of the amount of sand dropped onto the PDMS-coated mesh surface. The water contact angles before and after five repetitions of the sand abrasion test (20 g of fallen sand for each test) were almost identical (163.3° to 159.3°), indicating that the surface's superhydrophobicity was sustained after abrasion. By comparison to the surface morphology of the PDMS-coated mesh before the sand abrasion test (Fig. 4(c) and (d)), one can conclude that the surface of the PDMS-coated mesh was hardly altered by the sand abrasion test (Fig. 5(c)). In addition, another abrasion test was carried out with sand paper (Fig. S2). PDMS-coated mesh was faced and dragged on the sandpaper, which was repeated five times. Fig. S2(b) shows that the water contact angle after five repetitions of sand paper abrasion test was shown to be above 150°, which means that superhydrophobic film was maintained on the mesh surface. These results demonstrate the high mechanical stability of our PDMS-coated metal meshes.

To evaluate the photostability and chemical stability of the PDMS-coated mesh, it was exposed to UV light or acidic/basic aqueous solutions, and then the static water contact angle was measured after each treatment. When the mesh sample was irradiated with UV light for 12 h, the water contact angle of the mesh surface remained above 150° (Fig. 6(a)). In addition, when specimens of the PDMS-coated mesh were immersed in either an acidic (pH 2.5) or basic (pH 12) aqueous solution for 40 min, washed with distilled water and dried under atmospheric conditions, their water contact angles were still over 150°. These results reveal that the superhydrophobic surface on PDMS-coated mesh had good photo-resistance and chemical stability.

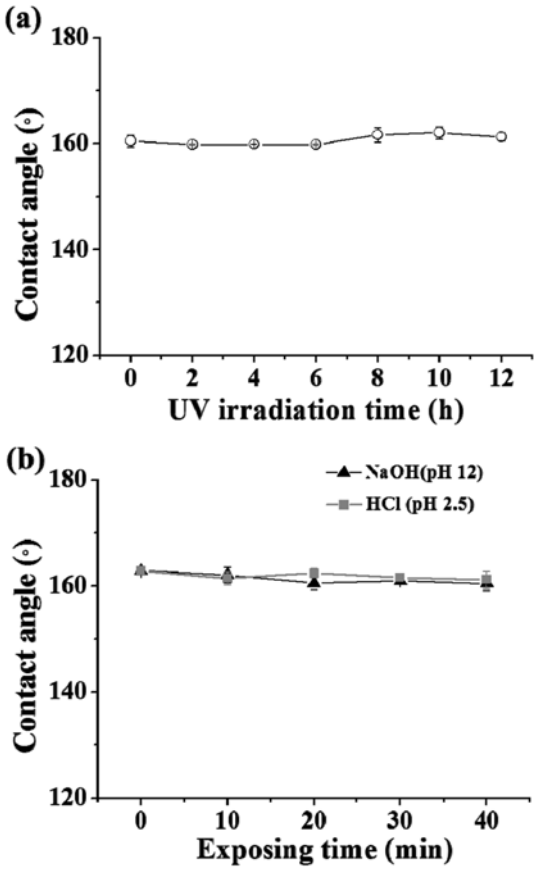

Fig. 6. Results of the photostability and chemical stability tests of PDMS-coated mesh: (a) water contact angle change of PDMS-coated mesh as a function of UV irradiation time. (b) water contact angles change of PDMS-coated mesh as a function of exposure time to acidic (HCl, pH 2.5) and basic (NaOH, pH 12) aqueous conditions.

3. Gas Permeation, Water Repellency, and Flexibility of PDMS-coated Mesh

A gas permeation and water repellency test of the PDMS-coated mesh was carried out using the simple setup shown in Fig. 7. During the injection of CO_2 gas into the branch, the clear $Ca(OH)_2$ aqueous solution gradually became hazy and the printed letters attached to the sidewall of the vial slowly became invisible (Fig. 7(a)), indicating that the CO_2 gas could penetrate the PDMS-coated mesh, allowing the precipitation of $CaCO_3$ from the aqueous solution.

Using the same experimental setup, a water repellency test of the

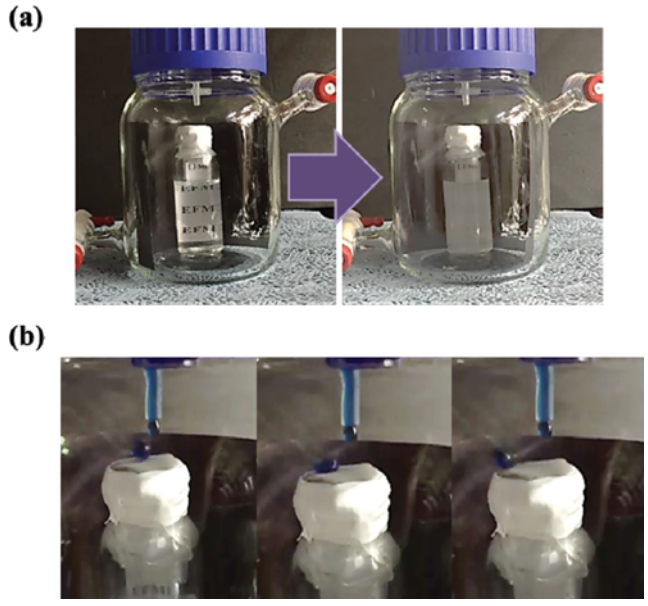

Fig. 7. (a) Images showing a vial containing $Ca(OH)_2$ solution before (left) and after (right) gas permeability test in glass reactor; (b) snapshots of a dyed water droplet bouncing on a PDMS-coated mesh during a water repellency test with syringe.

mesh was performed. When dyed aqueous solution was dropped on the PDMS-coated mesh using a syringe, the water droplet was observed to bounce off the mesh's surface (Fig. 7(b)). It was thus demonstrated that the PDMS-coated mesh is gas-permeable and superhydrophobic, allowing selective passage of the gas in gas/liquid mixtures. To demonstrate flexibility and endurance of superhydrophobic film, a bending test was performed Fig. 8(a) shows the good flexibility of PDMS-coated mesh. After repeated bending of the mesh, the water contact angles still were above 150° (Fig. 8(b)), which indicated that our sample was a flexible superhydrophobic film.

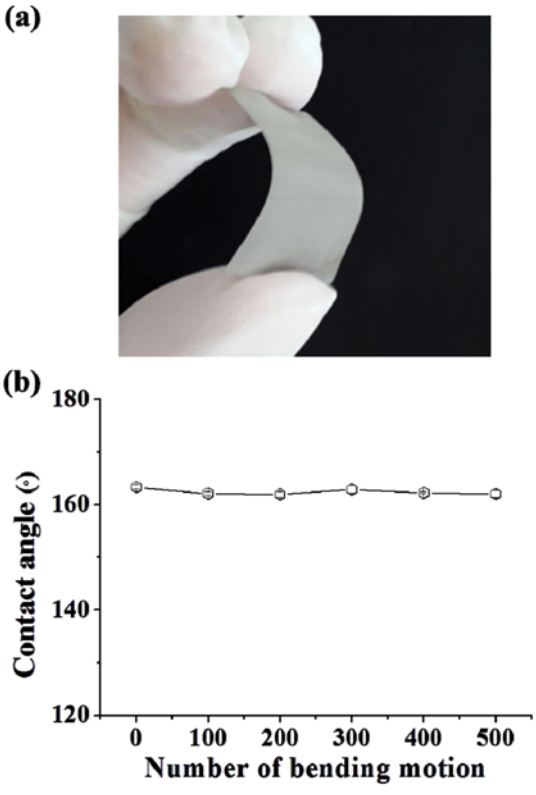

Fig. 8. (a) Image showing a flexibility of PDMS-coated mesh during bending motion; (b) change in water contact angle of PDMS-coated mesh as a function of number of bending motions.

CONCLUSIONS

We demonstrated a simple vapor deposition method for the preparation of gas-permeable, flexible superhydrophobic membranes based on metal mesh. The hierarchical surface structure formed by deposition of PDMS vapor resulted in a water contact angle exceeding 160°. A sand abrasion test showed that the superhydrophobicity of the PDMS-coated mesh was mechanically quite stable. The superhydrophobic surface on the mesh was also sustained after UV irradiation and acidic and basic treatments under aqueous conditions. We show that this PDMS-coated metal mesh is flexible, gas-permeable and superhydrophobic. We suggest that our PDMS-coated mesh has some potential for application in various fields; for example, in gas sensors, which can be easily contaminated by aqueous solutions, our mesh could act as a shielding layer, selectively filtering gas vapor (analyte) and protecting the sensor from the aqueous solutions. The mesh could also be used in buildings as water filters in air circulation systems, allowing the passage of gas while preventing the entry of rainwater [34,39-41] and application for oil-water filter, which means that our membrane can repel water and can trap oil [42-44].

ACKNOWLEDGEMENTS

This research was supported by the Civil–Military Technology Cooperation Program.

SUPPORTING INFORMATION

Additional information as noted in the text. This information is available via the Internet at http://www.springer.com/chemistry/journal/11814.

REFERENCES

1. B. Bhushan and Y. C. Jung, *Prog. Mater. Sci.*, **56**, 1 (2011).
2. E. Celia, T. Darmanin, E. Taffin de Givenchy, S. Amigoni and F. Guittard, *J. Collioid Interface Sci.*, **402**, 1 (2013).
3. T. Sun, L. Feng, X. Gao and L. Jiang, *Account Chem. Res.*, **38**, 644 (2005).
4. H. Teisala, M. Tuominen, M. Aromaa, M. Stepien, J. M. Mäkelä, J. J. Saarinen, M. Toivakka and J. Kuusipalo, *Langmuir*, **28**, 3138 (2012).
5. Y. Tian and L. Jiang, *Nat. Mater.*, **12**, 291 (2013).
6. T. Verho, C. Bower, P. Andrew, S. Franssila, O. Ikkala and R. H. A. Ras, *Adv. Mater.*, **23**, 673 (2011).
7. Z. Yoshimitsu, A. Nakajima, T. Watanabe and K. Hashimoto, *Lang-*

muir, **18**, 5818 (2002).
8. Y.-S. Cho, J. Moon, D. Lim and Y. Kim, *Korean J. Chem. Eng.*, **30**, 1142 (2013).
9. Z. Guo, W. Liu and B.-L. Su, *J. Collioid Interface Sci.*, **353**, 335 (2011).
10. A. Lafuma and D. Quere, *Nat. Mater.*, **2**, 457 (2003).
11. K. Liu, X. Yao and L. Jiang, *Chem. Soc. Rev.*, **39**, 3240 (2010).
12. Y. Lu, S. Sathasivam, J. Song, C. R. Crick, C. J. Carmalt and I. P. Parkin, *Science*, **347**, 1132 (2015).
13. B. J. Privett, J. Youn, S. A. Hong, J. Lee, J. Han, J. H. Shin and M. H. Schoenfisch, *Langmuir*, **27**, 9597 (2011).
14. H. Son, J. Park and W. Lee, *Korean J. Chem. Eng.*, **30**, 1480 (2013).
15. H. Zhou, H. Wang, H. Niu, A. Gestos and T. Lin, *Adv. Funct. Mater.*, **23**, 1664 (2013).
16. R. Fürstner, W. Barthlott, C. Neinhuis and P. Walzel, *Langmuir*, **21**, 956 (2005).
17. Y. Li, W. Cai and G. Duan, *Chem. Mater.*, **20**, 615 (2008).
18. J. A. Rogers and R. G. Nuzzo, *Mater. Today*, **8**, 50 (2005).
19. N. Gao and Y. Yan, *Nanoscale*, **4**, 2202 (2012).
20. B. J. Sparks, E. F. T. Hoff, L. Xiong, J. T. Goetz and D. L. Patton, *ACS Appl. Mater. Interfaces*, **5**, 1811 (2013).
21. C.-H. Xue and J.-Z. Ma, *J. Mater. Chem. A*, **1**, 4146 (2013).
22. S. M. Bawaked, S. Sathasivam, D. S. Bhachu, N. Chadwick, A. Y. Obaid, S. Al-Thabaiti, S. N. Basahel, C. J. Carmalt and I. P. Parkin, *J. Mater. Chem. A*, **2**, 12849 (2014).
23. C. R. Crick, J. C. Bear, A. Kafizas and I. P. Parkin, *Adv. Mater.*, **24**, 3505 (2012).
24. C. R. Crick, J. C. Bear, P. Southern and I. P. Parkin, *J. Mater. Chem. A*, **1**, 4336 (2013).
25. C. R. Crick, J. A. Gibbins and I. P. Parkin, *J. Mater. Chem. A*, **1**, 5943 (2013).
26. C. Edusi, G. Hyett, G. Sankar and I. P. Parkin, *Chem. Vapor Depos.*, **17**, 30 (2011).
27. E. J. Park, Y. K. Cho, D. H. Kim, M.-G. Jeong, Y. H. Kim and Y. D. Kim, *Langmuir*, **30**, 10256 (2014).
28. G. Liu, F. Xiangli, W. Wei, S. Liu and W. Jin, *Chem. Eng. J.*, **174**, 495 (2011).
29. Q. Chen, N. Miyata, T. Kokubo and T. Nakamura, *J. Mater. Sci.-Mater. M.*, **12**, 515 (2001).
30. A. P. D. P. J. Cotton, I. M. Graz and S. P. Lacour, *J. Appl. Phys.*, **109**, 54905 (2011).
31. K. M. McNamara, B. E. Williams, K. K. Gleason and B. E. Scruggs, *J. Appl. Phys.*, **76**, 2466 (1994).
32. M.-G. Jeong, H. Seo, K.-D. Kim, D. Kim, Y. Kim and D. Lim, *J. Mater. Sci.*, **47**, 5190 (2012).
33. K.-D. Kim, H. O. Seo, C. W. Sim, M.-G. Jeong, Y. D. Kim and D. C. Lim, *Prog. Org. Coat.*, **76**, 596 (2013).
34. E. J. Park, B. R. Kim, D. K. Park, S. W. Han, D. H. Kim, W. S. Yun and Y. D. Kim, *RSC Adv.*, **5**, 40595 (2015).
35. E. J. Park, K.-D. Kim, H. S. Yoon, M.-G. Jeong, D. H. Kim, D. C. Lim, Y. H. Kim and Y. D. Kim, *RSC Adv.*, **4**, 30368 (2014).
36. E. J. Park, J. K. Sim, M.-G. Jeong, H. O. Seo and Y. D. Kim, *RSC Adv.*, **3**, 12571 (2013).
37. B. Cortese, S. D'Amone, M. Manca, I. Viola, R. Cingolani and G. Gigli, *Langmuir*, **24**, 2712 (2008).
38. X. Liu, Y. Xu, Z. Chen, K. Ben and Z. Guan, *RSC Adv.*, **5**, 1315 (2015).
39. C. Feigley, J. Khan, D. Salzberg, J. Hussey, H. Attaway, L. Steed, M. Schmidt and H. Michels, *HVACR. RES.*, **19**, 53 (2012).
40. W. Tang, T. H. Kuehn and M. F. Simcik, *J. Occup. Environ. Hyg.*, **12**, 438 (2015).
41. T. Verdier, M. Coutand, A. Bertron and C. Roques, *Build. Environ.*, **80**, 136 (2014).
42. Q. Pan, M. Wang and H. Wang, *Appl. Surf. Sci.*, **254**, 6002 (2008).
43. C. Wang, T. Yao, J. Wu, C. Ma, Z. Fan, Z. Wang, Y. Cheng, Q. Lin and B. Yang, *ACS Appl. Mater. Interfaces*, **1**, 2613 (2009).
44. F. Wang, S. Yu, M. Xue, J. Ou and W. Li, *New J. Chem.*, **38**, 4388 (2014).

Supporting Information

Superhydrophobic, flexible and gas-permeable membrane prepared by a simple one-step vapor deposition

Bo Ra Kim, Dae Han Kim, and Young Dok Kim†

Department of Chemistry, Sungkyunkwan University, Suwon 16419, Korea
(*Received 7 November 2015 • accepted 17 January 2016*)

PDMS-coated mesh wrapped under bottom of material (40 g) was dragged on the sandpaper (2,000 mesh). The abrasion velocity and abrasion length are 2 cm·s^{-1} and 20 cm, respectively.

(a)

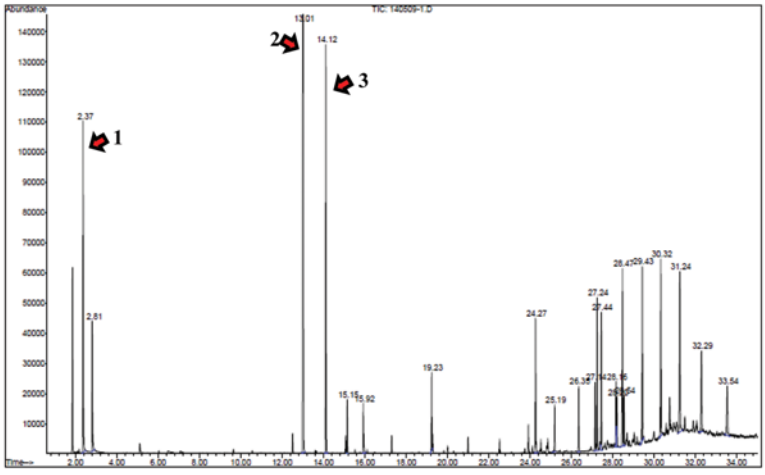

(b)

Peak No.	Area%	Molecular structure	Molecular weight
1	7.9	*tert*-Butyldimethylsilanol	132.3
		Silanol, trimethyl-	90.2
2	24.9	Pentasiloxane, dodecamethyl-	384.8
		Trisiloxane, 1,1,1,5,5,5-hexamethyl-3,3-bis[(trimethylsilyl)oxy]-	384.8
3	10.5	Cyclotetrasiloxane, octamethyl-	296.6

Fig. S1. (a) Pyrolysis gas chromatography data obtained from PDMS heated at 300 °C. (b) Molecular structures of major species in (a) are derived based on the mass spectrometry analyses.

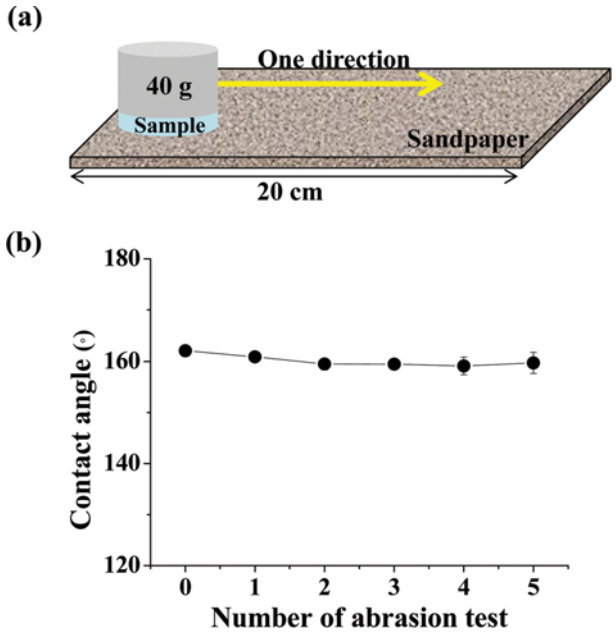

Fig. S2. (a) Schematic illustration of the experiment set-up for sandpaper abrasion test. (b) Change in water contact angle of PDMS-coated mesh as a function of number of sandpaper abrasion test.